



Published in final edited form as:

*J Biophotonics*. 2014 May ; 7(5): 281–285. doi:10.1002/jbio.201200220.

## Multispectral fluorescence lifetime imaging system for intravascular diagnostics with ultrasound guidance: *in vivo* validation in swine arteries

Julien Bec<sup>1</sup>, Dinglong M. Ma<sup>1</sup>, Diego R. Yankelevich<sup>1</sup>, Jing Liu<sup>1</sup>, William T. Ferrier<sup>2</sup>, Jeffrey Southard<sup>3</sup>, and Laura Marcu<sup>\*,1</sup>

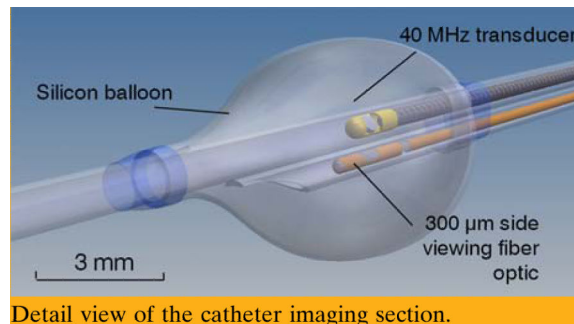
<sup>1</sup> University of California, Davis, Department of Biomedical Engineering, 451 Health Sciences Drive, CA, 95616, USA

<sup>2</sup> University of California, Davis, School of Medicine, Surgical Research Facility, One Shields Avenue, CA, 95616, USA

<sup>3</sup> University of California, Davis, Medical Center, Division of Cardiovascular Medicine, 4860 Y Street, Sacramento, CA 95817, USA

### Abstract

Fluorescence lifetime technique has demonstrated potential for analysis of atherosclerotic lesions and for complementing existing intravascular imaging modalities such as intravascular ultrasound (IVUS) in identifying lesions at high risk of rupture. This study presents a multimodal catheter system integrating a 40 MHz commercial IVUS and fluorescence lifetime imaging (FLIm) using fast helical motion scanning (400 rpm, 0.75 mm/s), able to acquire *in vivo* in pulsatile blood flow the autofluorescence emission of arterial vessels with high precision ( $5.08 \pm 0.26$  ns mean average lifetime over 13 scans). Co-registered FLIm and IVUS data allowed 3D visualization of both biochemical and morphological vessel properties. Current study supports the development of clinically compatible intravascular diagnostic system integrating FLIm and demonstrates, to our knowledge, the first *in vivo* intravascular application of a fluorescence lifetime imaging technique.



## Keywords

time resolved fluorescence spectroscopy; fluorescence lifetime imaging; intravascular ultrasound (IVUS); intravascular catheter; atherosclerosis

---

## 1. Introduction

Coronary artery disease is the leading cause of death in western societies [1]. Although many diagnostic tools have been developed to help predict which patients will suffer cardiovascular complications, current diagnostic techniques have significant limitations [2]. New techniques, including intravascular methods, are needed in order to make a significant impact on this public health challenge. Point time-resolved fluorescence spectroscopy (TRFS) and fluorescence lifetime imaging microscopy (FLIM) have demonstrated ability to assess a plurality of diagnostic features associated with arterial wall pathologies including atherosclerotic plaques at risk of rupture [3]. However, the overall TRFS and FLIM potential for atherosclerotic plaques analysis was primarily evaluated ex-vivo in arterial tissue specimens with intima directly exposed to the fiberoptic probe interrogation. Practical intravascular application of these techniques requires development of TRFS systems and catheters capable of rapid acquisition of robust time-resolved fluorescence data *in vivo* from the luminal surface of the artery in the presence of pulsatile blood flow. A novel implementation of a TRFS apparatus with the ability to rapidly ( $<1 \mu\text{s}$  per point measurement) spectrally and temporarily resolve tissue autofluorescence [4] has the potential to address such a problem. Using a fiberoptic for fluorescence excitation-collection coupled to this apparatus we demonstrated in tissue phantoms the potential of this approach for continuous recording in helical scanning (rotation and pull-back) of TRFS data from luminal surfaces in multiple spectral bands [5], thus enabling fluorescence lifetime imaging (FLIm) of the luminal surface. However, the slow, scanning speed of this apparatus (10 rpm, 0.01 mm/s) was found impractical for *in vivo* intravascular application.

The main goal of this study is to demonstrate how an improved version of this instrument allowed us to perform, to our knowledge, the first *in vivo* intravascular application of FLIm. The scanning parameters are compatible with intravascular clinical applications. A second goal is to conduct these experiments in conjunction with intravascular ultrasound (IVUS) which is the most commonly used intravascular imaging technique in patients [6]. In addition to guiding the TRFS measurement, IVUS provides complementary information on arterial morphology and anatomy. Thus, an intravascular rotational catheter combining FLIm with IVUS detection can provide a simultaneous evaluation of the biochemical and morphological features of the arterial vessels. In current study, we adapted a bi-modal catheter previously tested in tissue phantoms [7] to *in vivo* intravascular utilization and performed simultaneous acquisition of biochemical and structural features of arterial vessels.

## 2. Material and methods

The FLIm system was based on an adaptation of a multispectral TRFS system which principle is described elsewhere [4]. Briefly, a fiber laser (UV-Power355-0.2-PP, Fianium, UK) emitting 20 ps pulses at 355 nm with a fast repetition rate of 1 MHz is sending light to

the sample by mean of a UV-grade silica/ silica optical fiber with 300  $\mu\text{m}$  core (FVP300330360, Polymicro, Phoenix, AZ, USA). The fluence on tissue is below 35  $\text{mJ}/\text{cm}^2$ . The sample's autofluorescence is collected via the same fiber and is sent to a wavelength selection module (WSM) that splits the collected signal in four different channels with respective central wavelength/bandwidth of 390/40 nm (channel 1), 452/45 nm (channel 2), 542/50 nm (channel 3), and 629/53 nm (channel 4). Each sub-band is coupled into a delay fiber of different length and finally into a single multichannel plate photomultiplier (MCP-PMT, R5916U-50, Hamamatsu, Bridgewater, NJ, USA). The signal from the MCP-PMT is amplified by a preamplifier (C5594, 1.5 GHz bandwidth, Hamamatsu, Japan) and recorded by a fast digitizer (Acqiris U1065A, 3 GHz bandwidth, 8 GS/s sampling rate, Agilent, CA).

Intravascular FLIm was enabled by a custom 0.22 NA 300  $\mu\text{m}$  core silica side-viewing optical fiber (SVOF) connected to the WSM by mean of a custom fiber optic rotary joint (Doric Lenses, Quebec, Canada). The fiber, rotated using a brushless motor with an integrated controller (Maxon MCD EPOS, Sachseln, Switzerland), is inserted into an acrylic tubing (CT562-750-5, Paradigm Optics, WA).

The bimodal catheter is composed of the FLIm SVOF and a commercial 40 MHz IVUS 3 Fr catheter (Atlantis SR Pro, Boston Scientific, MA) coupled to an acquisition system (iLab, Boston Scientific, MA). The distal end of the SVOF was enclosed into a 1.5 mm inner diameter silicon tubing (SSF, Paso Robles, CA) that also covers part of the IVUS imaging section (Figure 1a). The IVUS sheath is fluorescent (405 nm peak emission,  $\sim 3.3$  ns lifetime) and was used as a reference fluorescent contrast marker. During the imaging sequence, the tube is inflated with saline until it seals the vessel. Fluorescence signal from the wall can then be acquired through the balloon without obstruction from blood. Both FLIm and IVUS are connected to a custom double translation stage allowing for axial alignment of IVUS and FLIm imaging planes and 6 mm length synchronized pull-back of IVUS transducer and SVOF into the catheter sheath.

The capability of this multimodal system to acquire *in vivo* bimodal data of arteries was tested in a swine model, in compliance with the UC Davis Institutional Animal Care and Use Committee. A 62 kg pig was induced for general anesthesia with telazol, intubated, ventilated, and placed on isoflurane maintenance anesthesia. Local anesthesia was given with 1% lidocaine and the femoral artery was surgically exposed using standard cutdown techniques. After direct visualization of the artery a needle was placed into the front wall of the artery using a modified Seldinger technique. Subsequent dilation of the artery lead to placement of a 9 Fr sheath. IV heparin was given to maintain adequate anti coagulation. An 0.014" guide-wire was introduced into the femoral artery under fluoroscopic guidance. The bimodal catheter was then placed on the guide and inserted to the area to be imaged. A total of 13 bimodal scans were acquired from 3 distinct arterial locations.

The image acquisition sequence was subdivided into a preliminary phase relying on real time IVUS image display where an artery section was chosen based on diameter (measured by IVUS) and the balloon was inflated, and a data acquisition sequence where the area of interest was scanned. The frame rate for FLIm was 5 KHz with eight consecutive

measurements being averaged. The SVOF was rotated at 400 rpm with a 0.75 mm/s pullback speed over a 6 mm pullback length, providing 3.8° angular sampling and 110 mm axial sampling. The IVUS was rotated at 1800 rpm with a similar pullback speed, providing 1.4° angular sampling and 24 mm axial sampling. The duration of the imaging sequence was 12 s (4 s for initial balloon inflation, 8 s for data acquisition). Each FLIm frame, containing the fluorescence decay corresponding to the four channels (Figure 2a, top), had a duration of 250 ns and was sampled at 8 GHz using simultaneous acquisition and read-out method. This technique allows acquisition of up to 35,000 consecutive frames (7 s duration at maximum frame rate). Both FLIm and IVUS data were then processed and co-registered as previously reported [7, 8]. Briefly, the signal of the fluorescence decay was analyzed to obtain a series of fluorescence intensity and average lifetime values for each channel. The intensity value at each point was obtained by integrating over time the fluorescence decay for this point. The fluorescence impulse response function (fIRF) was calculated using a least-square deconvolution technique based on Laguerre basis expansion [8]. The measured fluorescence pulse is a convolution of the fIRF with the instrument impulse response function, determined experimentally. The average lifetime value  $\tau_{avg}$  is calculated according to the following equation where the fIRF is noted as  $\hat{h}(k)$ :

$$\tau_{avg} = \frac{\delta t \sum_{k=0}^{N-1} k \hat{h}(k)}{\sum_{k=0}^{N-1} \hat{h}(k)}.$$

An example of fitted data is presented in Figure 2a. The corresponding two-dimensional co-registered images were then created by matching each point measurement with the spatial sampling obtained from each modality acquisition frequency and scanning parameters. Figure 1b presents a typical co-registered FLIm lifetime and IVUS data. We can observe the position of the IVUS transducer, the SVOF and its shadow, the vessel wall fluorescence signal (in red) but also a low lifetime area (in green) which corresponds to the fluorescence from the IVUS transducer. Such co-registration requires axial and angular alignment. The axial alignment is trivial as both modalities share the same imaging plane. Angular alignment was achieved using features in the images as both shadows should be positioned at 180° from each other. For each frame the vessel lumen was manually segmented from the IVUS image. The value of each pixel of the vessel surface was obtained by interpolating data corresponding to this axial and angular position from the 2D FLIm image. This was repeated for each IVUS frame; the registered frames were then processed using Amira (VSG, Burlington, MA) to obtain the co-registered 3D images (Figure 1b).

### 3. Results

The experiment was carried out on a healthy pig so the vessel wall should be uniform. The IVUS transducer as seen by the SVOF provides contrast in the FLIm image. Figure 2b and c present the fluorescence intensity and average lifetime for two distinct acquisitions in 6 mm and 3 mm diameter vessels. Variations in the fiber-to-tissue distance cause significant variations of signal amplitude across the intensity images. On the other hand, lifetime

images are rather uniform in the areas corresponding to both vessel wall and IVUS transducer.

The corresponding histograms of intensity and average lifetime over the field of view are shown in Figure 2d and e. The intensity histogram does not present noticeable features; differences between cases are mainly due to variations of collection geometry. Lifetime histograms present two peaks at  $3.5 \pm 0.37$  ns and  $5.1 \pm 0.26$  ns corresponding to the average lifetime values of the arterial wall and IVUS sheath, respectively. To evaluate the average lifetime distribution within vessel and transducer areas, the lifetime images were segmented and their spread analyzed. Figure 2f presents individual results for six arterial scans where a good separation of lifetime values between “vessel” and “transducer” groups is observed. Additionally, the mean fluorescence average lifetime values across 13 scans was determined at  $5.08 \pm 0.26$  ns for the vessel and  $3.47 \pm 0.37$  ns for sheath, showing consistent measurements across all scanning acquisitions.

#### 4. Discussion and conclusion

The FLIm derived spectroscopic images acquired intravascularly in pulsatile blood flow demonstrated the ability of this technique to rapidly ( $\sim 8$  s per 0.6 cm arterial segment length) and consistently resolve the autofluorescence features of arterial wall. FLIm images show consistent fluorescence lifetime values for the normal arterial vessel which is dominated by elastin and collagen fluorescence emission as well as the transducer fluorescent sheath which was used here as contrast marker (Figure 2b and c). As expected, the measured arterial wall fluorescence lifetime ( $\sim 5$  ns) was similar to values previously reported for healthy pig arteries when using similar methods for analysis of fluorescence decay [5, 7]. The lifetime images also allowed for a clear delineation of areas corresponding to other fluorescent structures such as the transducer sheath (Figures 2b and c). Notably, in contrast, the intensity images show significant variations over the scanned area, making difficult to distinguish features (Figure 2c). This result underscores the robustness of lifetime measurements from tissues with respect to changes in light excitation-collection geometry typical of measurements in dynamic environments.

The IVUS played an important role in identifying the arterial regions of interest and in real-time measurement of vessel diameter. Moreover, as seen in Figure 1b the IVUS and FLIm data can be co-registered to provide straightforward bimodal image display.

Current FLIm system allowed imaging of arterial vessels as small as 3 mm diameter requiring only brief ( $< 12$  s) balloon occlusion making this device compatible with intravascular procedures.

A more practical application of this technique will require reduction in size ideally down to  $\sim 3$  Fr in the imaging section. Further development of a co-axial FLIm-IVUS catheter will allow not only for reduction in catheter diameter but also for an increased angular field of view (no shadowing between channels). Such design would greatly enhance the functionality of the system.

The fluence on tissue ( $35 \text{ mJ/cm}^2$ ) is higher than the maximum permissible exposure (MPE) for skin of  $14 \text{ mJ/cm}^2$  computed according to ANSI standard using the laser and scanning parameters. It can be lowered well below the MPE limit by using a laser repetition rate that matches the system acquisition rate (5 KHz).

In summary, the bimodal FLIm-IVUS system reported here represent a key milestone towards the development of clinically compatible multimodal intravascular diagnostic systems integrating FLIm as it allowed, to our knowledge, the first *in vivo* intravascular application of a helical scanning fluorescence lifetime imaging technique.

## Acknowledgements

This study was supported by the NIH Grant R01 HL 67377. The IVUS system used in this study was made available by Boston Scientific Corporation.

## References

1. Lloyd-Jones D, Adams R, Carnethon M, De Simone G, Bruce Ferguson T, Flegal K, Ford E, Furie K, Go A, Greenlund K, Haase N, Hailpern S, Ho M, Howard V, Kissela B, Kittner S, Lackland D, Lisa-beth L, Marelli A, McDermott M, Meigs J, Mozaffarian D, Nichol G, O'Donnell C, Roger V, Rosa-mond W, Sacco R, Sorlie P, Stafford R, Steinberger J, Thom T, Wasserthiel-Smoller S, Wong N, Wylie-Rosett J, Hong Y. the American Heart Association Statistics Committee and Stroke Statistics Subcommittee. *Circulation*. 2009; 119:480–486. [PubMed: 19171871]
2. Suter MJ, Nadkarni SK, Weisz G, Tanaka A, Jaffer FA, Bouma BE, Tearney GJ. *JACC: Cardiovascular Imaging*. 2011; 4:1022–1039. [PubMed: 21920342]
3. Marcu L. *Journal of Biomedical Optics*. 2010; 15:011106. [PubMed: 20210432]
4. Sun Y, Sun Y, Stephens D, Xie H, Phipps J, Saroufeem R, Southard J, Elson DS, Marcu L. *Opt. Express*. 2011; 19:3890–3901. [PubMed: 21369214]
5. Xie H, Bec J, Liu J, Sun Y, Lam M, Yankelevich DR, Marcu L. *Biomed. Opt. Express*. 2012; 3:1521–1533. [PubMed: 22808425]
6. Honda Y, Fitzgerald PJ. *Circulation*. 2008; 117:2024–2037. [PubMed: 18413510]
7. Bec J, Xie H, Yankelevich DR, Zhou F, Sun Y, Ghata N, Aldredge R, Marcu L. *Journal of Biomedical Optics*. 2012; 17:106012. [PubMed: 23224011]
8. Liu J, Sun Y, Jinyi Q, Marcu L. *Physics in Medicine and Biology*. 2012; 57:843–865. [PubMed: 22290334]

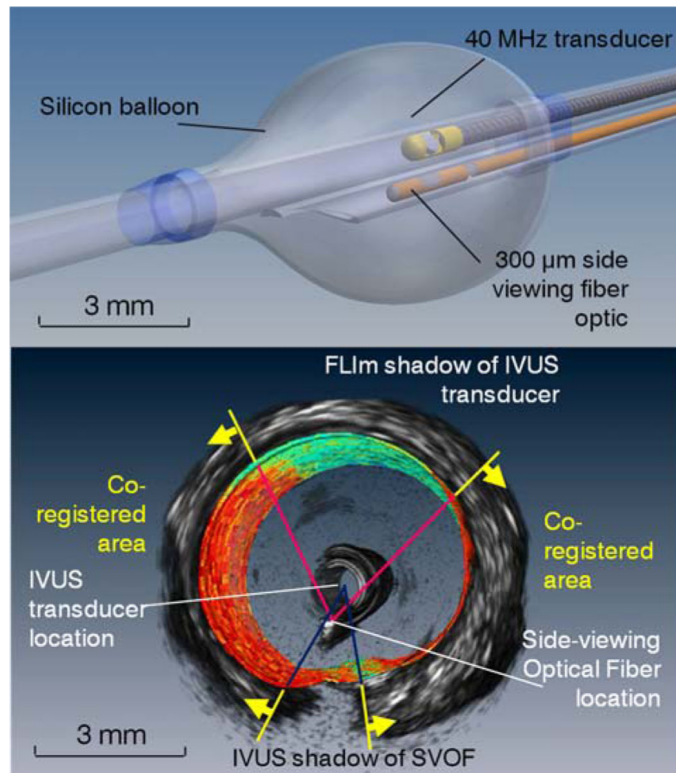


**Figure 1.** (a) Detail view of the catheter imaging section; (b) 3D FLIm and IVUS co-registered image showing locations of the fiber and IVUS, respective shadowing and effectively co-registered area of the vessel between yellow arrows.



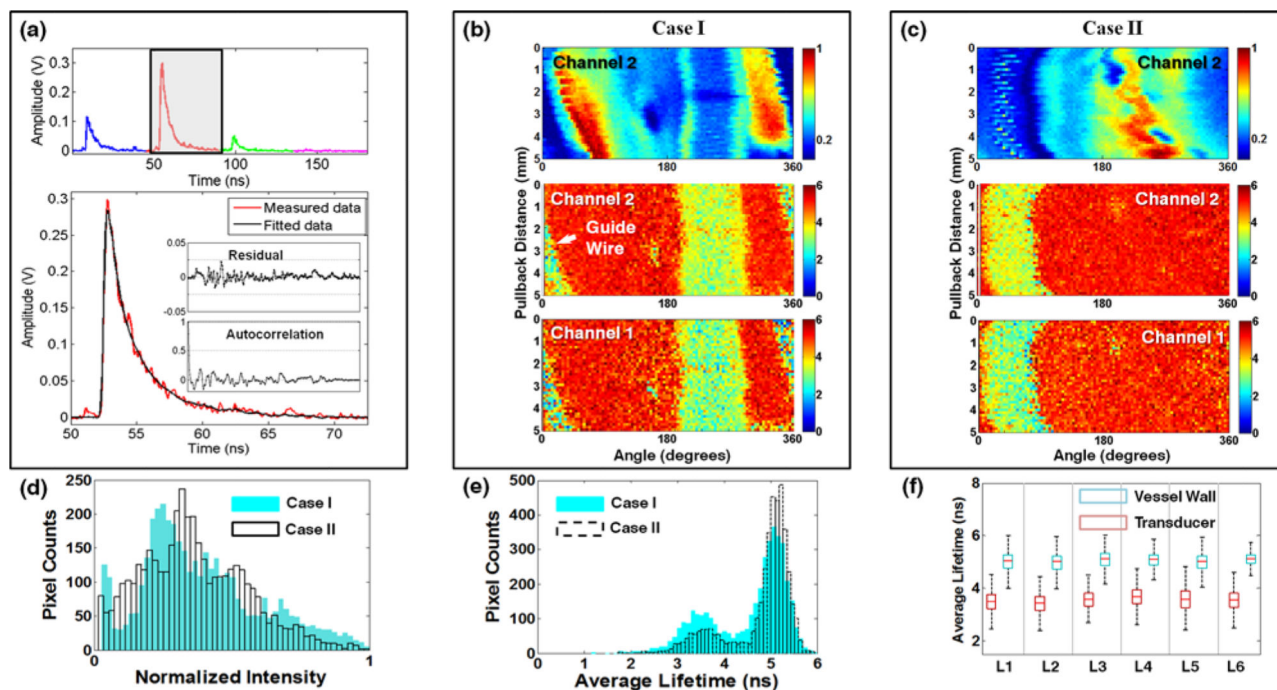


**Figure 2.** *in vivo* FLIm measurements of pig vessel at multiple locations. (a) Raw data showing measured decays at one point for all 4 channels (top) and deconvolved decay (bottom) for Channel 2. (b) and (c) Representative FLIm data from two locations, case 1 (diameter ~6 mm) and case 2 (diameter ~3 mm): from top to bottom, Channel 2 (450 nm) normalized intensity and average lifetime and Channel 1 (390 nm) average lifetime. Each pixel has a dimension of  $110 \mu\text{m} \times 3.8^\circ$ . (d) Normalized fluorescence intensity histograms from Case 1 and Case 2. (e) Average lifetime histograms from Case 1 and Case 2. (f) Representative cases of average lifetime values distribution from vessel wall and transducer at six acquisitions (L1 to L6) from three distinct locations.